# A Simple and Low Cost Micromixer for Laminar Blood Mixing: Design, Optimization, and Analysis

Nhut Tran-Minh[1,2,*], Frank Karlsen[1], Tao Dong[1], and Hai Le-The[1]

[1] Vestfold University College, Postboks 2243, N-3103 Tonsberg, Norway
[2] Norchip AS, Industriveien 8, N-3490 Klokkarstua, Norway
{Nhut.Tran-Minh,Frank.Karlsen,Tao.Dong}@hive.no,
Hai.Le.The@student.hive.no

**Abstract.** The paper presents a design of micromixer for laminar blood mixing. In order to minimize the space usage for micromixer of an automatic sample collection system, a splitting and recombination (SAR) concept was employed to reduce the diffusion distance of the fluids. Moreover, ellipse-like micropillars were introduced to this concept to increase the mixing performance of micromixer. With software (COMSOL 4.3) for computational fluid dynamics (CFD) we simulated the mixing of fluids in a micromixer with ellipse-like micropillars and basic T-type mixer in a laminar flow regime. Numerical results illustrate that the micromixer with SAR concept achieves an outstanding mixing efficiency than the one without SAR concept. Numerical results also show that the SAR micromixer with ellipse-like micropillars is up to 99% efficient, and that efficiency reaches 90% in a short distance.

**Keywords:** Micromixer, passive mixing, splitting and recombination, MEMS.

## 1 Introduction

The main vision for the future clinical diagnostics using self-sampling procedure in homes or health rooms, include automatic, painless and large volume collection of blood sample. This is to secure representative sample, optimal user abilities, proper skin and blood vain handling and sustainable prevention health operations. However, before large whole blood volumes may be handled it is important to manage automatic, painless and small volume of whole blood from the finger for quick point-of-care diagnosis. An automatic sample collection module with a painless microneedle array in combination with a micromixer is proposed for the blood collection in typical nurse or health rooms (Fig.1).

In general, micromixers can be classified into active micromixer and passive micromixer. In the mixing process, active micromixers require external disturbance effects such as pressure, temperature, electrohydrodynamics, dielectrophoretics, electrokinetics, etc. Hence, the structures of active micromixers are often complicated. In contrast to active micromixer, a passive type requires no external energy. The normal mixing process within a passive micromixer is slow and entirely dependent upon

* Corresponding author.

T.D. Pham et al. (Eds.): ACBIT 2013, CCIS 404, pp. 91–104, 2014.

molecular diffusion [1-3]. The mixing of the passive microfluidic mixer is based on several main principles: a) flow laminar, which is used in the T-mixer [3-4]; b) chaotic mixing by eddy formation [5]; c) splitting and combination [6]. Previous studies of micromixer [6-9] show that fast and homogenous mixing can be achieved in the micromixer with SAR concept by increasing the contact interface of fluids. But some of them are complicated and require complex microfabrication processes because of their three dimensional micro structure [1].

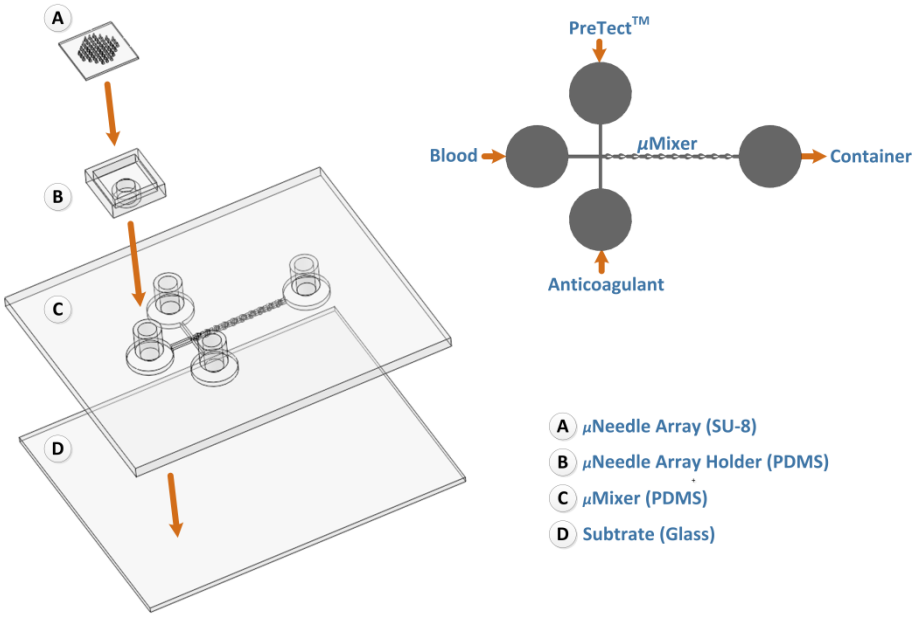


**Fig. 1.** Painless sample collection systems

In this paper, a simple and low cost splitting and recombination micromixer with ellipse-like micropillars was investigated. The efficiency of the micromixer was examined by theoretical methods including Finite Element Method (FEM). Simulation results are presented with the laminar flow regime, in which a low Reynolds number is applied, $0.048 \leq Re \leq 2.381$.

## 2 Micromixer Design

The term ellipse-like micropillar is an element having the shape of an ellipse. As shown in Fig.2, a contour of the micropillar was described as an ellipse with the left major axis semidiameter $a_1$, right major axis semidiameter $a_2$, and minor axis semidiameter $b$. It should be noted that the high velocity region along the two sides of the contour was larger when the length of the left half axis $a_1$ is not equal to that of the right half axis $a_1$, that is $a_1 < a_2$. The optimized values of the profile parameters are $a_1 : a_2 : b = 5 : 6 : 4$ [10].

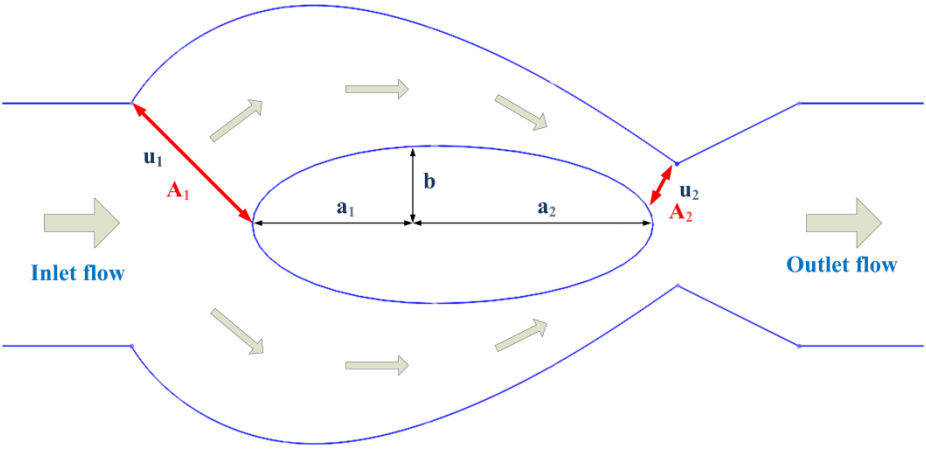


**Fig. 2.** Mixing unit of SAR micromixer

Due to the demand for fast and homogenous mixing, the splitting and recombination concept is considered in blood mixer design. There are three steps in splitting and recombination process, flow splitting, flow recombination and flow rearrangement [2]. When the main flow reaches the ellipse-like micropillar, the flow is then split into two separated flows on the smaller channels. For an incompressible fluid, equation of continuity (mass conservation of fluid) is defined as [11]

$$A_1 u_1 = A_2 u_2 \tag{1}$$

Since cross-section area $A_2$ is less than cross-section area $A_1$ (see Fig.2), the local velocity $u_2$ will be larger than velocity $u_1$. This phenomenon together with the high velocity region of ellipse-like micropillar will create high velocity at the right end of the micropillar's contour. At the outlet end of the micropillar, two separated flows in small channels are recombined with high velocity. The contact interface of fluids is increased throughout each mixing unit so that the mixing effect is enhanced.

SAR micromixer ellipse-like micropillars for blood mixing includes 3 inlet channels (blood sample, anticoagulant solution, Pretect™ solution (NorChip, Klokkarstua, Norway)), one outlet channel, and some mixing units. The geometry of SAR micromixer with ellipse-like micropillars is shown in Fig.3.

Whole blood undergoes coagulation few seconds after it has left the *in vivo* condition [12]. Therefore, the whole blood has to undergo immediate mixing with the right concentration of EDTA (Trysin-EDTA-solution, Sigma-Aldrich Co. LLC) after it has left the body. In addition the whole blood has to be mixed with a weak fixative (PreTect™, Klokkarstua, Norway) that is ideal for long term conservation of DNA, protein and RNA at room temperature [13]. The degradation process of the RNA starts just a few seconds after the blood has left the host organism [14]. Therefore, it is very important to secure optimal mixing between both the PreTect™ medium and the Heparin (EDTA solution). In this way optimal amplification and detection will follow optimal sample preparation and RNA/DNA/Protein purification/extraction.

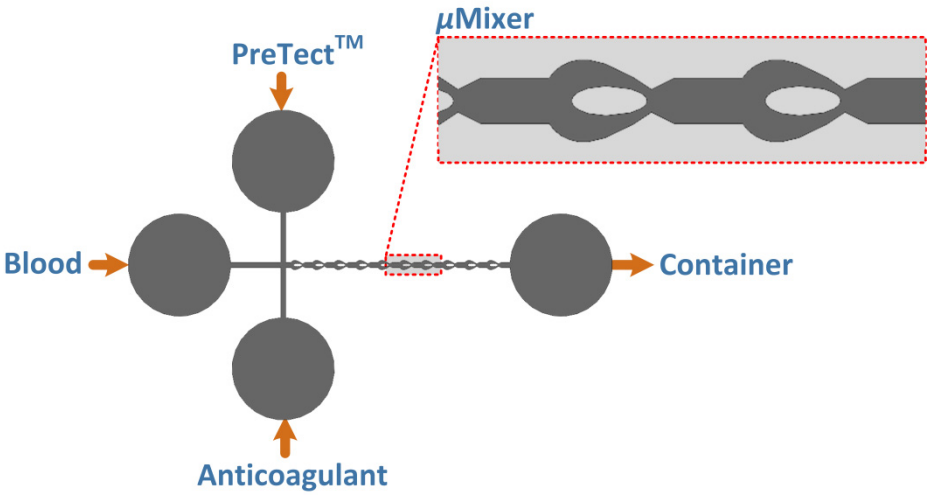


**Fig. 3.** SAR micromixer for blood mixing

## 3 Theoretical Analysis of Micromixer

The flow in SAR micromixer can generally be described by the Navier-Stokes equation and continuity equation as shown in Eqs (2) and (3), respectively.

$$\frac{\partial u}{\partial t} + u \cdot \nabla u = -\frac{1}{\rho}\nabla p + \nu \nabla^2 u \tag{2}$$

$$\nabla \cdot u = 0 \tag{3}$$

in which appear velocity $u$, density $\rho$ of the fluid, pressure $p$, and kinematic viscosity $\nu$ of the fluid.

The species transport in the systems can be described by the diffusion-convection equation as shown in Eq. (3).

$$\frac{\partial c}{\partial t} + (u \cdot \nabla)c = D\nabla^2 c \tag{4}$$

where $c$ and $D$ are concentration and diffusion constant of the species, respectively.

The variables for the mixing studies are the flow rate corresponding to the characteristic dimensionless number $Re$ (Reynolds number) and number of mixing units in SAR micromixer. The Reynolds number is defined as

$$Re = \frac{uL_c}{\nu} \tag{5}$$

where $Re$ represent the ratio between momentum and viscous friction, $L_c$ indicate the characteristic length of the flow.

The Reynolds number is the factor to determine the flow regime. The flow is considered to be turbulent flow when the Reynolds number is greater than 4000. For a Reynolds number falling below 2300, the flow is considered as laminar flow. In the macro scale, a Reynolds number of greater than 4000 can be easily achieved. In microdevice, the Reynolds number rarely exceeds 2000 [3]. Hence, the mixing in microchannel is based on molecular diffusion.

It is essential to consider another characteristic dimensionless number $Pe$ (Peclet number), in order to investigate the efficiency of the SAR micromixer. Peclet number is defined as

$$Pe = \frac{uL_c}{D} \tag{6}$$

where $Pe$ represents the ratio between the mass transport due to convection and diffusion. From Eq. (5) and (6), relation between $Pe$ and $Re$ can be derived as

$$\frac{Pe}{Re} = \frac{\nu}{D} = \frac{\mu}{\rho D} \tag{7}$$

where $\mu$ is the dynamic viscosity of the fluid.

For comparison purposes, water was used as the carrier fluid, so that the dynamic viscosity, density, and the diffusion coefficient of fluid at room temperature (25oC) are $0.001 kg.s/m$, $1000 kg/m^3$, and $10^{-9} m^2/s$, respectively. Hence, the relation between $Pe$ and $Re$ can be estimated for water as $Pe$ = 1000 $Re$. The transverse diffusion time can be estimated by the following equation:

$$t = \frac{{L_c}^2}{D} \tag{8}$$

Therefore, the characteristic mixing length of micromixer to obtain the complete mixing is

$$L = ut = u\frac{{L_c}^2}{D} = Pe\, L_c \tag{9}$$

Eq. (9) indicates that the higher is the Peclet number, the more difficult will be to achieve a complete mixing. Therefore, in the laminar flow regime ($Re$ value is lower than 2300), the higher $Re$ value makes the mixing less efficient.

## 4 CFD Modeling and Setting

The geometric size and configuration of SAR micromixer with ellipse-like micropillar is shown in Fig.4. The micromixer consists of three inlets and one outlet, with a mixing unit length 450μm. The simulated SAR micromixer with 10 ellipse-like micropillars has a total length 10mm. The depth of micromixer is 500μm.

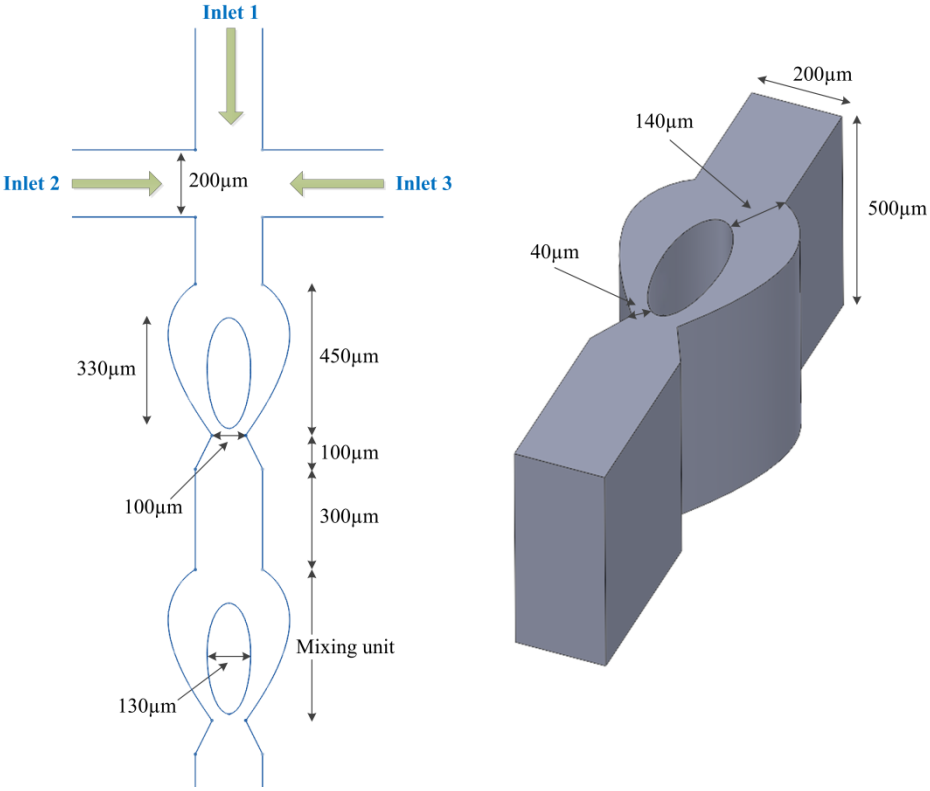


**Fig. 4.** Schematic illustration of the SAR micromixer with ellipse-like micropillars geometry and configuration

Multiphysics simulation software (COMSOL 4.3) was used to examine the mixing performance of the basic T-mixer and SAR micromixer with ellipse-like micropillars. During simulation, the incompressible steady flow condition was assumed. The physical properties of water were applied and the diffusion coefficient of the water-ink mixture is $3.23\times10^{-10}$ $m^2s^{-1}$ [15]. No-slip condition is applied to the boundary on the wall. The fixed velocity was set to three inlets. The fixed pressure ($p = 0$) was set to the outlet of the micromixer. The normalized molar concentration of the species was set 1 for inlet 1, 0 for inlet 2 and inlet 3. To investigate the mixing process, simulations were performed at ten flow rates as listed in Table 1.

**Table 1.** Flow rate and $Re$ value of numerical simulation

| Flow Inlet (ml/min) | Velocity (m/s) | Reynolds number | Peclet number |
|---|---|---|---|
| 0.005 | 0.00083 | 0.2381 | 238.1 |
| 0.010 | 0.00167 | 0.4762 | 476.2 |
| 0.015 | 0.00250 | 0.7143 | 714.3 |
| 0.020 | 0.00333 | 0.9524 | 952.4 |
| 0.025 | 0.00417 | 1.1905 | 1190.5 |
| 0.030 | 0.00500 | 1.4286 | 1428.6 |
| 0.035 | 0.00583 | 1.6667 | 1666.7 |
| 0.040 | 0.00667 | 1.9048 | 1904.8 |
| 0.045 | 0.00750 | 2.1429 | 2142.9 |
| 0.050 | 0.00833 | 2.3810 | 2381.0 |

## 5 Post Processing

To evaluate homogeneity of the fluid, the variance of the concentration is considered in the simulation.

$$\sigma^2 = \frac{1}{N}\sum_{i=1}^{N}({c^*}_i - \overline{c^*})^2 \tag{10}$$

where $N$ is the total number of sampling points, ${c^*}_i$ and $\overline{c^*}$ are normalized concentration and expected normalized concentration, respectively.

In the evaluation process of variance of the concentration, characteristic dimensionless parameter $z'/Pe$ should be included.

$$\frac{z'}{Pe} = \frac{z}{L_c}\frac{D}{uL_c} = \frac{z/u}{{L_c}^2/D} = \frac{t_{flow}}{t_{diffusion}} \tag{11}$$

Thus the parameter $z'/Pe$ is a ratio of the time for flow in the axial direction to the time for diffusion in the transverse direction.

The variance of the concentration can be normalized again by mean concentration and taken square root to evaluating the mixing index:

$$\gamma = \sqrt{\frac{1}{N}\sum_{i=1}^{N}\left(\frac{{c_i}^* - \overline{c^*}}{\overline{c^*}}\right)^2} \tag{12}$$

The mixing index $\gamma$ presents perfect mixing with value 0 and no mixing with the value 1. Mixing efficiency of the micromixer can be calculated by the formula as follow:

$$\eta = 1 - \gamma = 1 - \sqrt{\frac{1}{N}\sum_{i=1}^{N}\left(\frac{c_i^* - \overline{c^*}}{\overline{c^*}}\right)^2} \tag{13}$$

Mixing efficiency ranges from 0.00 (0% mixing) to 1 (100% mixing, full mixed). The efficiency between around 80% and 100% is acceptable for mixing process application.

## 6 Results and Discussion

### 6.1 Mixing Field and Performance

Fig.5 shows that the mixing process of the Fluid 1 (red) and Fluid 2, 3 (dark blue) in the SAR micromixer with 10 ellipse-like micropillars ($Re$=0.714). The concentration field was normalized such that the concentration of Fluid 1 denoted a value 1; the concentration of Fluid 2 and Fluid 4 denoted a value 0. We defined that the mixing region having a concentration between 0.23 and 0.43. The larger is the mixing region, the better mixing are the fluids. In the flow downstream, three fluids contacted each other vertically and suffered the effects of separation, recombination by the designed structure. Hence, the mixing region was increased.

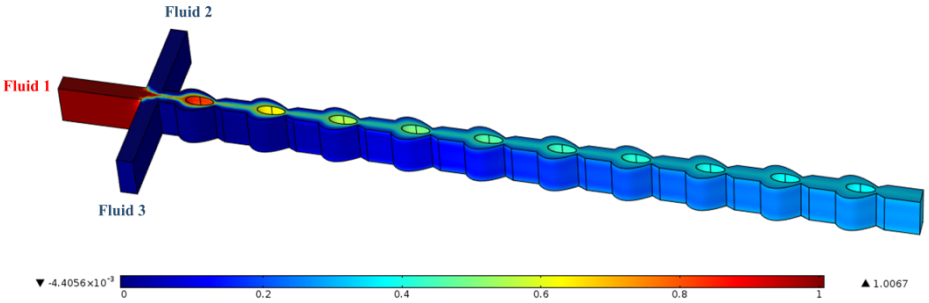


**Fig. 5.** Fluid mixing in SAR mixer with 10 mixing units from CFD simulation ($Re$ = 0.714)

In order to investigate the action of splitting and recombination, the basic T-mixer was chosen to compare with SAR-mixer with 10 mixing units. The basic T-mixer had a main channel of depth 500µm and width 200µm. The total length of both T-mixer and SAR-mixer are 10mm. Fig.6 shows the concentration of the fluid in T-mixer and SAR mixer with 10 mixing units at various Reynolds numbers. The color of the fluids clearly varied with the increase in mixing distance. For $Re$ = 0.714, the fluids were mixed well in short distance. For higher Reynolds number, mixing region in SAR-mixer is larger than mixing region in T-mixer. It is due to the presence of ellipse-like micropillars in mixing channel. Flowing downstream, the fluids mixed rapidly to exhibit a uniform light blue. For $Re$ = 1.429, the fluid was completely mixed in SAR mixer, whereas mixing of the fluids in T-mixer was incomplete.

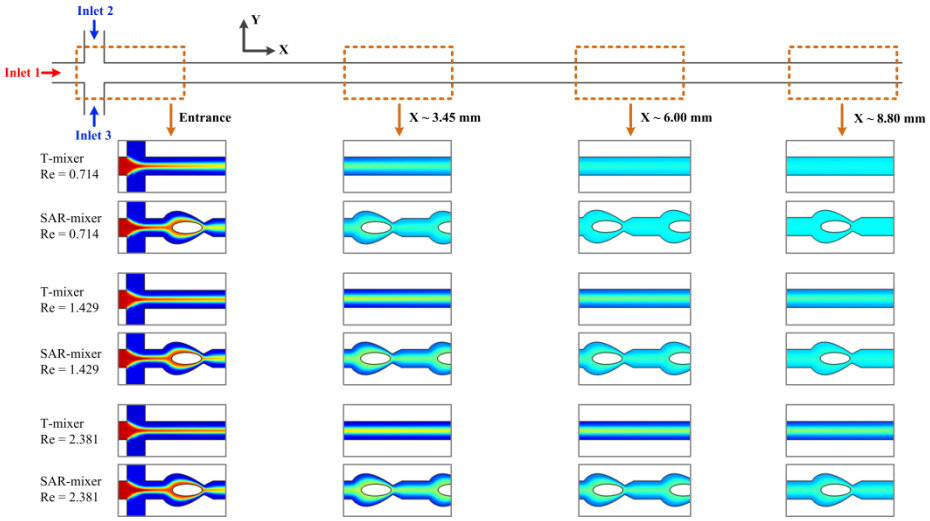


**Fig. 6.** Visualization of fluid mixing in T-mixer and SAR-mixer

## 6.2 Mixing Efficiency

At low Reynolds number, mixing process takes place in microchannel through molecular diffusion. Fig.7 and Fig.8 illustrate the variance of concentration in term of characteristic dimensionless parameter $z'/Pe$. In order to depict these diagrams, numerical simulation in COMSOL 4.3 were carried out with various flow rates. Hence, each diagram will represent the mixing behavior of each micromixer. Then they can be used to examine which kind of micromixer is better.

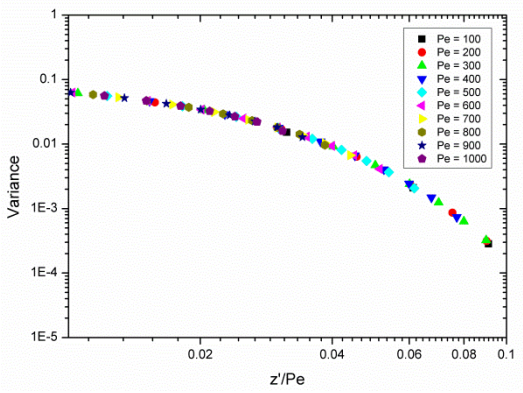


**Fig. 7.** Variance of mixing of micromixer without mixing unit

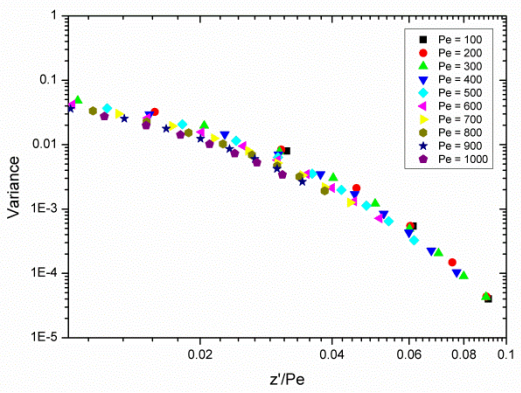


**Fig. 8.** Variance of mixing of micromixer with 10 mixing units

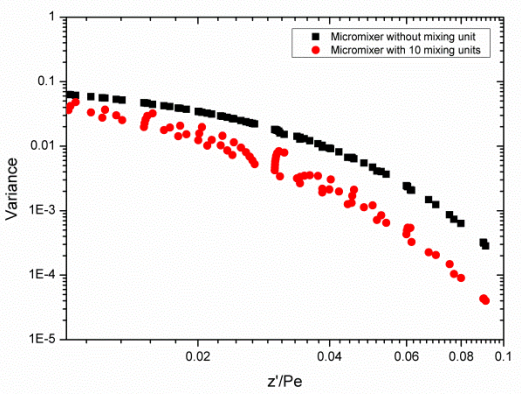


**Fig. 9.** Comparison of concentration's variance between T-mixer and SAR-mixer

Fig.9 shows the comparison of the concentration's variance between T-mixer (black squares) and SAR-mixer (red circles). It obviously shows that no matter how far the mixing length or how large the flow rate, variance of concentration in SAR-mixer is always lower than the variance of concentration in SAR-mixer. Furthermore, for the same flow rate at the inlets (same Peclet number), variance of concentration in the SAR mixer after distance 8.58mm ($z' = 30$, $L_c$= 285µm, $Pe = 1000$) is equal to the variance of concentration in T-mixer after distance 14.25mm ($z' = 50$, $L_c$ = 285µm, $Pe = 1000$). Thus, the SAR-mixer is suitable to minimize the space usage for micromixer on the automatic sample collection module.

Fig. 10 shows the mixing efficiency of T-mixer (no mixing unit) and SAR-mixer with varied number of mixing units on various cross-sections (different distance from the inlet) at $Re = 0.714$. Mixing efficiency of 0 (0%) denoted that the mixing fluids were not mixed at all. In basic T-mixer, the fluids were not mixed well at the outlet of the channel when its mixing efficiency is 0.7471 (74.71%) lower than the critical value of well mixing (80%). SAR-mixer with 10 mixing units reaches a critical value of well mixing after 6mm. When $Re$ value was increased to 2.381, mixing efficiency

of all mixers is lower than the critical value of well mixing (Fig.11). It means that, the length for well mixing was increased when $Re$ value was increased, see Eq.(9).

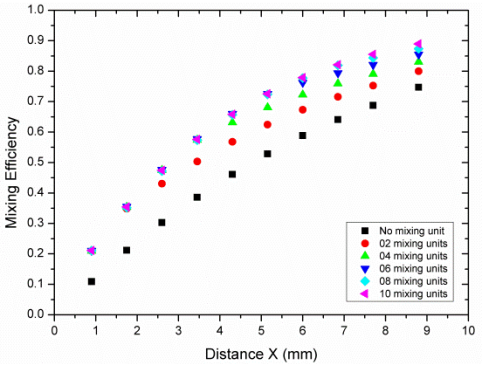


**Fig. 10.** Comparison of efficiency at $Re$ = 0.714

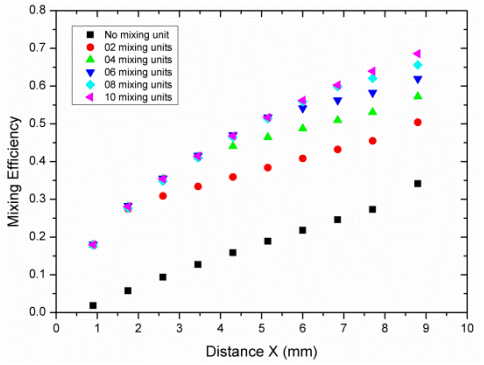


**Fig. 11.** Comparison of efficiency at $Re$ = 2.381

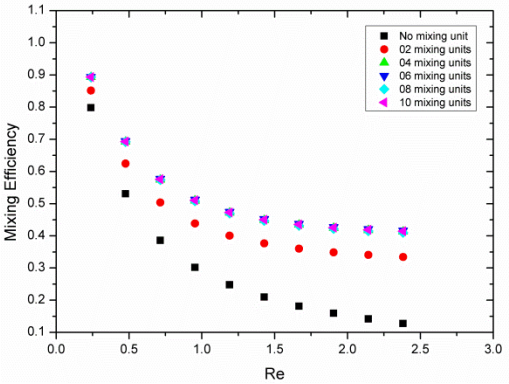


(a) After 3450µm

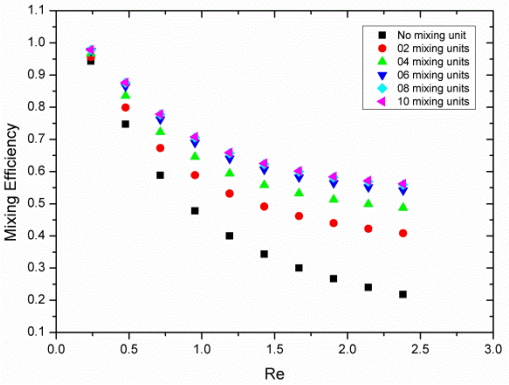


(b) After 6000µm

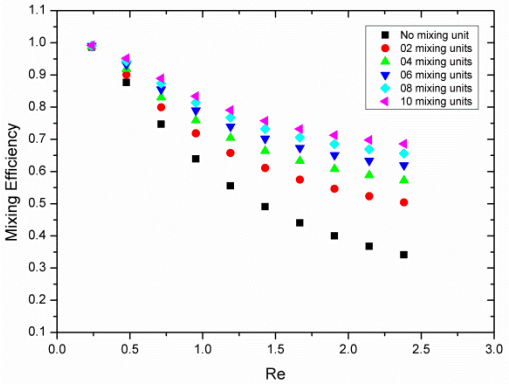


(c) After 8800µm

**Fig. 12.** Comparison of efficiency after different distances

Fig. 12 illustrates mixing efficiency in term of Reynolds number. As the figures show, the mixing efficiency drops as $Re$ increases, but the rate of decrease in SAR mixer is lower than T-mixer (no mixing unit). It should be noted that mixing efficiency is about 80% or more at $Re \leq 1$, which is suitable for mixing application. Fig. 12(c) shows that the mixing efficiency of SAR micromixer with 10 mixing unit after 8.8mm is always higher than 80% when $Re \leq 1$, whereas the mixing efficiency of the basic T-mixer is not acceptable when $Re > 0.5$. It means that fluids need to flow so slow in basic T-mixer in order to obtain the well mixed status. In SAR mixer, fluids flow faster for rapid mixing and mixing efficiency is still higher than the critical value for well mixing.

## 7 Conclusions

A splitting and recombination micromixer with ellipse-like micropillars has been proposed and investigated by FEM. Numerical results show that micromixer with ellipse-like micropillars have a well mixing status when its mixing efficiency is higher than 80% as $Re \leq 1$. This micromixer improved the performance of previous micromixer (T-mixer) at a low Reynolds number. Moreover, this kind of micromixers may be ideal for a user friendly, rapid and optimal collection and mixing related sample preparation of whole blood or any other complex human or biological fluidics used for point-of-care or point-of-need diagnostic applications and technologies.

**Acknowledgments.** This research work is supported by the Research Council of Norway and Norchip AS (Norway). The travel grant for presenting research work at the international conference is supported by the Research Council of Norway through the Norwegian PhD Network on Nanotechnology for Microsystems, contract no. 190086/S10.

## References

1. Nguyen, N.T., Wu, Z.: Micromixers—a review. J. Micromech. Micro eng. 16, R1–R16 (2005)
2. Hessel, V., Lowe, H., Schonfeld, F.: Micromixers—a review on passive and active mixing principles. Chemical Engineering Science 60, 2479–2501 (2005)
3. Bhagat, A.A.S., Peterson, E.T.K., Papautsky, I.: A passive planar micromixer with obstructions for mixing at low Reynolds numbers. J. Micromech. Microeng. 17, 1017–1024 (2007)
4. Wong, S.H., Ward, M.C.L., Wharton, C.W.: Micro T-mixer as a rapid mixing micromixer. Sensors and Actuators B 100, 359–379 (2004)
5. Nguyen, T.N.T., Kim, M., Park, J., Lee, N.: An effective passive microfluidic mixer utilizing chaotic advection. Sensors and Actuators B 132, 172–181 (2008)
6. Lee, S.W., Kim, D.S., Lee, S.S., Kwon, T.H.: Split and recombination micromixer based on PDMS three-dimensional micro structure. In: The 13th International Conference on Solid-State Sensors, Actuators and Microsystems, Seoul, Korea, June 5-9, pp. 1533–1536 (2005)

7. Lee, S.W., Lee, S.S.: Rotation effect in split and recombination micromixing. Sensors and Actuators B 129, 364–371 (2008)
8. Fanga, W., Yang, J.: A novel microreactor with 3D rotating flow to boost fluid reaction and mixing of viscous fluids. Sensors and Actuators B 140, 629–642 (2009)
9. Chen, Z., Bown, M.R., O'Sullivan, B., MacInnes, J.M., Allen, R.W.K., Mulder, M., Blom, M., van't Oever, R.: Performance analysis of a folding flow micromixer. Microfluid. Nanofluid. 6, 763–774 (2009)
10. Tran-Minh, N., Dong, T., Su, Q., Yang, Z., Jakobsen, H., Karlsen, F.: Design and optimization of non-clogging counter-flow microconcentrator for enriching epidermoid cervical. Biomed. Microdevices 13, 179–190 (2011)
11. Currie, I.G.: Fundamental Mechanics of Fluids. McGraw-Hill, Inc., New York (1993)
12. Handley, A.J.: Heparin therapy: A simpler test of control. J. Clin. Path. 27(3), 250–252 (1974)
13. Dixon, E.P., Grønn, P., King, L.M., Passineau, H., Doobay, H., Skomedal, H., Hariri, J., Hay, S.N., Brown, C.A., Fischer, T.J., Malinowski, D.P.: Analytical performance of RNA isolated from BD SurePath™ cervical cytology specimens by the PreTect™ HPV-Proofer assay. Journal of Virological Methods 185(2), 199–203 (2012)
14. Burka, E.R.: Characteristics of RNA degradation in the erythroid cell. J. Clin. Invest. 48(7), 1266–1272 (1969)
15. Lee, S., Lee, H.-Y., Lee, I.-F., Tseng, C.-Y.: Ink diffusion in water. Eur. J. Phys. 25, 331–336 (2004)